COMPARING THE OSTEOGENIC AND BONE REGENERATIVE CAPACITIES OF MTA, NANO MTA, NANO HYDROXYAPATITE AND INJECTABLE PLATELET RICH FIBRIN IN A RAT BONY DEFECT MODEL. AN IN VIVO STUDY

Hajer M. Abd Elhamid[*], Dina Rady[**] *and* Fatma M. Abu Naeem[***]

ABSTRACT

Aim: To compare the bone regenerative capacity of Bulk MTA formula with that of a nanoform of MTA (Nano MTA), nanohydroxyapatite (Nano HA) and injectable platelet rich fibrin (i-PRF) in a rat bony defect model.

Materials and methods: 100 male adult albino rats were anesthetized and a bone defect was created in the right tibiae. The rats were randomly divided into two groups according to dates of scarification (7 and 21 days), which were in turn subdivided into five sub-groups with ten animals each based on the defect filled by: Nano MTA, Nano hydroxyapatite, i-PRF, Bulk MTA and empty defect as control. All the right tibiae were dissected for histological analysis and histomorphometric measurements to assess bone regeneration in the defect area. Bone area percentage (%) were calculated.

Results: New bone formation was observed in all sub-groups. On day 7, histological analysis revealed partially filled defects with woven bone trabeculae with variable trabecular pattern enclosing fibro-cellular tissue spaces containing blood capillaries and collagen fibers. On day 21, all experimental groups showed newly formed mature bone, including the presence of organized osteocytes and reversal lines indicating bone remodeling. Histomorphometric analysis revealed that statistically important differences between bone formations in all treated sub-groups in comparison to the untreated control sub-group in both interval times (P<0.001). However, an increase in the bone area percentage was observed throughout the experimental periods in all sub-groups without statistical difference.

Conclusion: Within the limitations of the present experiment, it could be concluded that Nano MTA induced the most favorable tissue response and osteopromotion properties followed by Nano HA and i-PRF compared with conventional MTA. Although the results are very encouraging, more studies on i-PRF properties are mandatory before routine clinical use.

KEY WORDS: MTA, Nanohydroxyapatite, Injectable platelet rich fibrin, Bone regeneration.

* Lecturer of Endodontics, Endodontic Department, Faculty of Dentistry, MTI University.
** Lecturer of Oral biology, Oral biology Department, Faculty of Dentistry, Cairo university
*** Lecturer of Endodontics, Endodontic Department, Faculty of Dentistry, Cairo University.

INTRODUCTION

A major problem in managing a variety of endodontic cases is the isolation of the operative field for moisture control specially when dealing with critical cases such as pulp capping cases, perforation repair and endodontic surgery with the need for a perfect retrograde seal [1].

For these purposes Torabinejad and colleagues [2] developed a bioactive material known as Mineral Trioxide Aggregate which is ideal in sealing communications between the root canal system and the oral cavity such as mechanical and carious pulp exposures and between the root canal system and the periodontium such as perforations, open apices, resorptive defects, root-end preparations [1,3]. MTA is biocompatible with the capacity to stimulate regeneration of hard tissue and osteogenesis, and is hydrophilic that sets perfect in the presence of moisture [4,5]. MTA consists of fine trioxides (Tricalcium oxide, Silicate oxide, Bismute oxide) and other hydrophilic particles (Tricalcium silicate, Tricalcium aluminate) that sets in the presence of moisture by hydration reaction [1,6].

Calcium phosphates such as hydroxyapatite (HA) are composed of the same ions as the main mineral content of bone, they are biocompatible, osteoconductive with great hard tissue regenerative power, and produce no systemic toxicity or immunological reactions [7-9].

Nanotechnology is rapidly growing due to its favorable effect on the properties of materials producing superior properties from the same material increasing the sealing and antibacterial properties of variety of endodontic materials [10].

Injectable Platelet rich fibrin concentrate is obtained from autologous blood. It has a great importance because it contains high numbers of cells including leukocytes prior to the formation of a fibrin clot [11]. It was shown that I-PRF was able to release higher amounts of growth factors such as PDGF, TGF-β1, VEGF, EGF, and IGF when compared to ordinary PRF and PRP which directs the process of hard tissue repair by acting as signaling molecules with a great impact on the cell migration, proliferation, differentiation, matrix synthesis and mineralization in addition to angiogenic stimulation and proliferation of osteoblasts [12-17].

So, the aim of this study is to compare the osteogenic and bone regenerative capacity of original MTA formula with that of a nanoform of MTA, nanohydroxyapatite and i-PRF in a rat bony defect model.

MATERIALS AND METHODS

Study design and Animal grouping

One hundred rats were randomly distributed into 2 groups according to two time points of scarification dates, 7 days and 21 days. Then the animals were randomly allocated to one of five sub-groups (n=10 per sub-group) according to the material used for bone defect reconstruction as follow:

Sub-group A: tibia defect model treated with ***Nano MTA***.

Sub-group B: tibia defect model treated with ***Nano HA***.

Sub-group C: tibia defect model treated with ***i-PRF***.

Sub-group D: tibia defect model treated with ***Bulk MTA***.

Sub-group E: tibia defect left empty as **control**

Materials:

Material preparation:

Preparation of Nano MTA

Nano MTA was synthesized by sol gel method where the calcium nitrate, followed by aluminum nitrate was dissolved in 180 ml water, under

magnetically stirring, until a clear solution was obtained. TEOS was hydrolyzed where the molar ratio of TEOS: water was 1:4. The clear solution was continuously stirred at 60°C for 4 hours, then kept for the next 96 hours at 70°C, to facilitate the water evaporation and to accelerate the polycondensation reaction which resulted in the formation of a viscous gel. This gel was then dried at 120°C for 420 hours and the final product was a white powder. The powder was pressed in pellets and thermally treated at 1200°C for 30 minutes. Rapid cooling of the thermally treated material was performed in air.

Preparation of i-PRF

Approximately 10 ml of venous blood was drawn by intracardiac aspiration of the rat and transferred to a sterile plastic tube without anticoagulant which was immediately centrifuged using a tabletop centrifuge at 700 rpm for 3 min at room temperature [18]. The top of the tube translucent yellow (avoiding aspiration of the fraction of red blood cells) was collected as i-PRF. The i-PRF was then injected inside the bony defect using a plastic syringe.

Preparation of Nano HA

Hydroxyapatite nanoparticles was prepared by wet chemical method where Hydroxyapatite nanoparticles was formed through the wet chemical reaction of calcium nitrate, with ammonium hydroxide $((NH4)_2HPO_4)$. The grain size was controlled by changing the time and the temperature of HA precipitation, with pH values between 10 and 12 and the reaction was performed at room temperature.

Bulk MTA

Matreva white MTA was used (Matreva, Egypt)

Animals:

One hundred adult male albino rats weighting approximately 200±25 gm were used. They were obtained from the animal house, Faculty of Medicine, Cairo University.

Surgical protocol:

Surgical procedures were performed under general anesthesia with a combination of ketamine chlorhydrate (0.08 mL/100 g body weight) and xylazine 2% (0.04 mL/100 g body weight) [19].

Under sterile conditions, the right tibiae were disinfected with iodate alcohol and shaved. A 2 cm incision was made in the skin in the medial direction until exposure of the proximal end of the tibia. The periosteum was elevated and direct approach to the rat tibiae was attained. A 3 mm in diameter bone defect was created using a trephine surgical bur size 3 coupled to a low-speed hand piece connected to a micro-motor with 2000 rpm under constant irrigation with saline solution to prevent the overheating of bone margins until the medullary canal was reached (Fig.1). All materials were placed in the medullary cavity in the bone defect area and covered with the sutured periosteum to prevent leakage of the materials. All the procedures were performed by the same surgeon, previously trained.

The muscle and fascia were then repositioned, the muscular layer was sutured with resorbable #4.0 catgut and the skin was sutured with interrupted #4.0 silk sutures
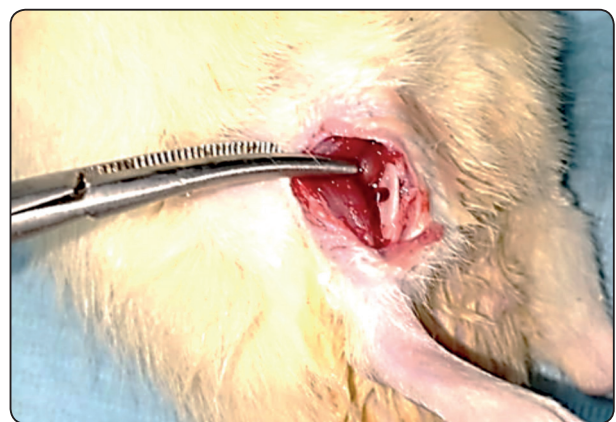

Fig. (1) A photomicrograph showing rat tibial bone defect

Postoperative care of the animals:

Upon completion of the surgical procedure, each animal received a single dose of cefazolin sodium, 50 mg/kg by intramuscular injection [19]

Housing and husbandry:

Animals were housed in the animal house, Faculty of Medicine, Cairo University under the supervision of a specialized veterinarian. Animals were kept in separate cages and maintained under controlled temperature at $25°C \pm 2°C$ with 12 h light/dark cycle.

Animals were fed standard rats chow and water with good ventilation condition throughout the experiment.

Animal sacrifice:

The animals were euthanized with an intra-cardiac overdose of sodium thiopental at 7 days and 21 weeks after the experiment was carried out. All tibiae were dissected free from any soft tissues; the bone specimens of each group were cut by a disc under constant irrigation to include the entire defect sites.

Specimens processing and data collection

Bone healing assessment:

Bone healing at the bone defect area was assessed as follows:

a) Histological examination by Haematoxylin and Eosin stain (H & E).

Histological samples were fixed in 10% formalin for 72 hours and decalcified in 10% ethylenediamine tetraacetic acid (EDTA) solution (for decalcification) for approximately 2 months. After complete decalcification, dehydration was carried out in a graded alcohol series, and the samples were embedded in paraffin blocks. Transverse sections

of 4–5 μm thickness were prepared for each tibia defect. All slices were stained with hematoxylin and eosin. Histological examination of the slides was carried out using a light microscope equipped with eyepiece at x400 magnification.

b) Histomorphometric analysis of the retrieved samples

The bone area percent of the newly formed bone in the region of bone repair for each specimen was measured using Leica Owen 500 image analyzer Computer system connected to a colored video camera, colored monitor, hard disc of IBM personal computer connected to the microscope and controlled by Leica Qwen 500 software. This optical system was associated with a histometry software package with image-capturing capabilities (Image J software)[20,21].

Statistical analysis:

The statistical calculations were carried out with the SPSS software package, version 15.0 (SPSS Inc., Chicago, IL, USA) for Windows. Results for descriptive statistics were expressed as mean ± standard deviation (SD). Statistical comparisons of continuous and multiple variables among the groups were performed using ANOVA and Student t test statistical significance was observed between groups. P-values less than 0.05 was considered as statistically significant.

RESULTS

Postoperatively, the rats recovered quickly, returning to routine activities such as grooming, eating and drinking in less than 48 hrs. Regardless of the implanted material there were no signs of inflammation or bone graft material rejection in any of the experimental groups.

I) Histological results:

Histological analysis revealed all bony defects

were partially filled with newly formed bone which was characterized by the presence of thin, interconnected or not and varied trabecular pattern in all sub-groups seven days postoperatively (Fig. 2A-E). Traces of the graft materials were seen in isolated areas in the experimental groups, and the particles were surrounded by a fibrous tissue layer (Fig. 2A, B & D). In the experimental groups; the defects were filled with woven bone with intervening fibro-cellular tissue containing blood capillaries and collagen fibers. Osteoblasts could be detected rimming the borders of the woven bone. The newly formed bone appeared basophilic, indicating less mineral content which were formed of cellularized woven bone displaying randomly distributed osteocytes located in wide lacunae. In Nano MTA sub-group, there were woven bone trabeculae interconnecting with each other, harboring wide marrow cavities in between them containing remnants of the material. In addition, there was recruitment of osteoblasts within the granulation tissue around the woven bone trabeculae (Fig. 2A). In Nano HA sub-group, the bone defects were filled with woven bone trabeculae which were in grown between the grafted materials, sometimes showing the presence of irregular osteocytes and rimming of osteoblasts (Fig. 2B). i-PRF sub-group revealed well-developed vascularization and mesh-like pattern of newly formed bone, that all together fully filled the defects. Notably, the new bone was highly cellular (Figs. 2C). In Bulk MTA sub-group, woven bone trabeculae characterized by the presence of globules or thin interconnecting bone trabeculae with wide marrow cavities, many osteocytes in their wide lacunae and osteoblasts rimming the surface (Fig. 2D). While in the control sub-group, a fibrous tissue occurred around at the edges of

the defect, granulation tissue appeared filling the bony defect. A combination of spindle cells with elongated nuclei and small rounded cells with large nuclei were detected in the connective tissue. Few irregularly distributed spicules of woven bone were seen together with the granulation tissue. Area of active bone resorption was observed with several osteoclast cells residing in Howship's lacunae at the old bone margin sites (Fig. 2E).

On 21 days, all experimental groups showed newly formed bone with characteristics of mature bone in some areas, including the presence of much more organized osteocytes with the formation of cavities filled with hematopoietic tissue. However, young immature bone was noted in other areas. Reversal lines were noted indicating bone remodeling (Fig. 3A-E). In Nano MTA sub-group, thicker bone trabeculae and narrower marrow cavities were noticed. Lacunae containing osteocytes were also frequent. Endosteum was observed (Fig. 3A). In Nano HA sub-group, the defects were repaired with newly formed bone characterized by trabecular bone tissue of variable thickness, enclosing osteocytes, surrounding marrow cavities enclosing well vascularized connective tissue (Fig. 3B). Remnants of graft material were still noticed surrounded by fibro-cellular tissue in the bone defect (Fig. 3A & 3B). In i-PRF sub-group, there were areas where bone trabeculae displayed few osteocytes alternating with other areas containing intense osteocytic infiltration (Fig. 3C). In Bulk MTA sub-groups revealed newly formed bone that exhibited irregularly distributed osteocytes located in relatively wide lacunae (Fig. 3D). While in the control sub-group defect sites, fewer new bone trabeculae lined with active osteoblast enclosing wide marrow cavities (Fig. 3E).
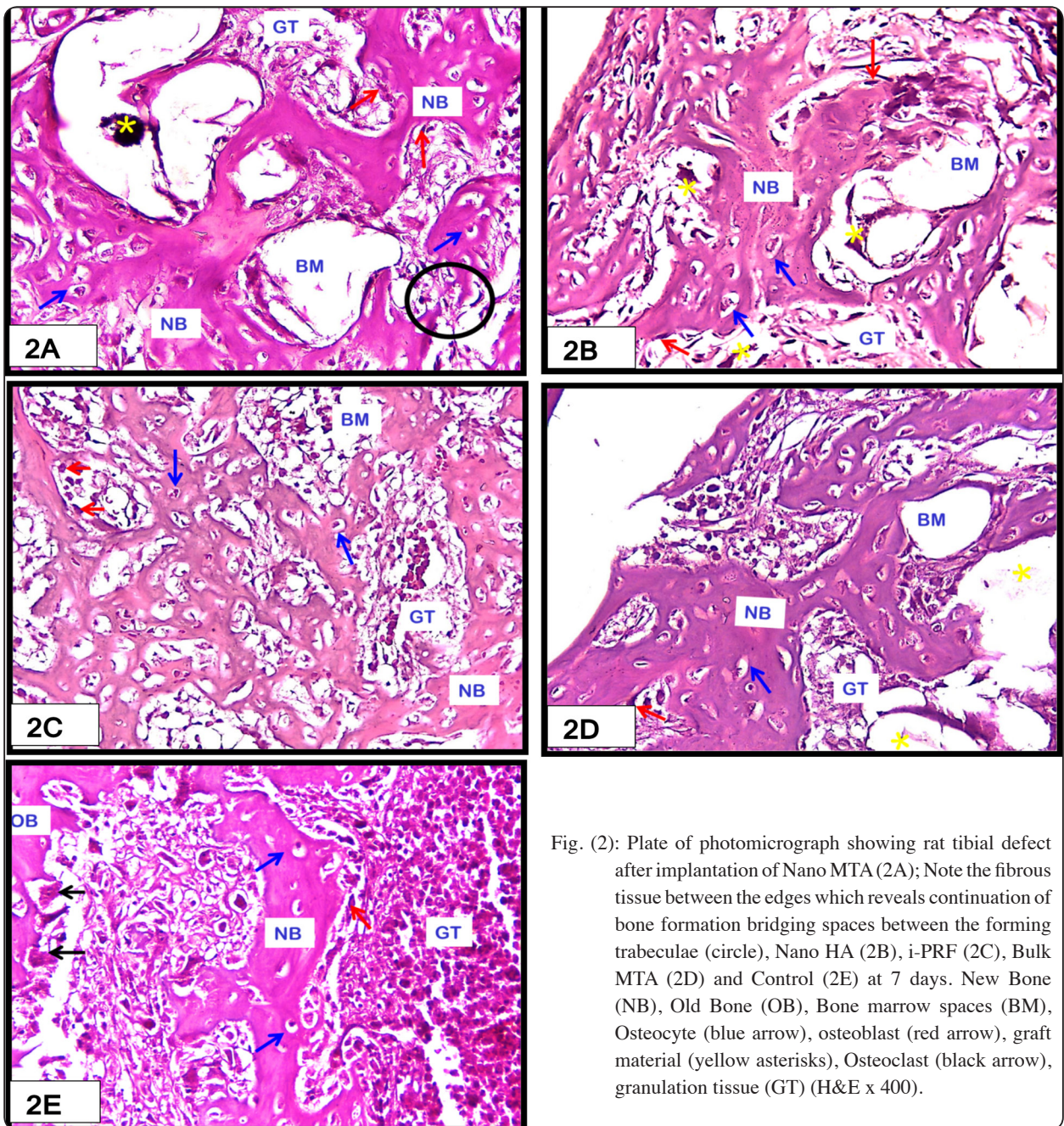
Fig. (2): Plate of photomicrograph showing rat tibial defect after implantation of Nano MTA (2A); Note the fibrous tissue between the edges which reveals continuation of bone formation bridging spaces between the forming trabeculae (circle), Nano HA (2B), i-PRF (2C), Bulk MTA (2D) and Control (2E) at 7 days. New Bone (NB), Old Bone (OB), Bone marrow spaces (BM), Osteocyte (blue arrow), osteoblast (red arrow), graft material (yellow asterisks), Osteoclast (black arrow), granulation tissue (GT) (H&E x 400).
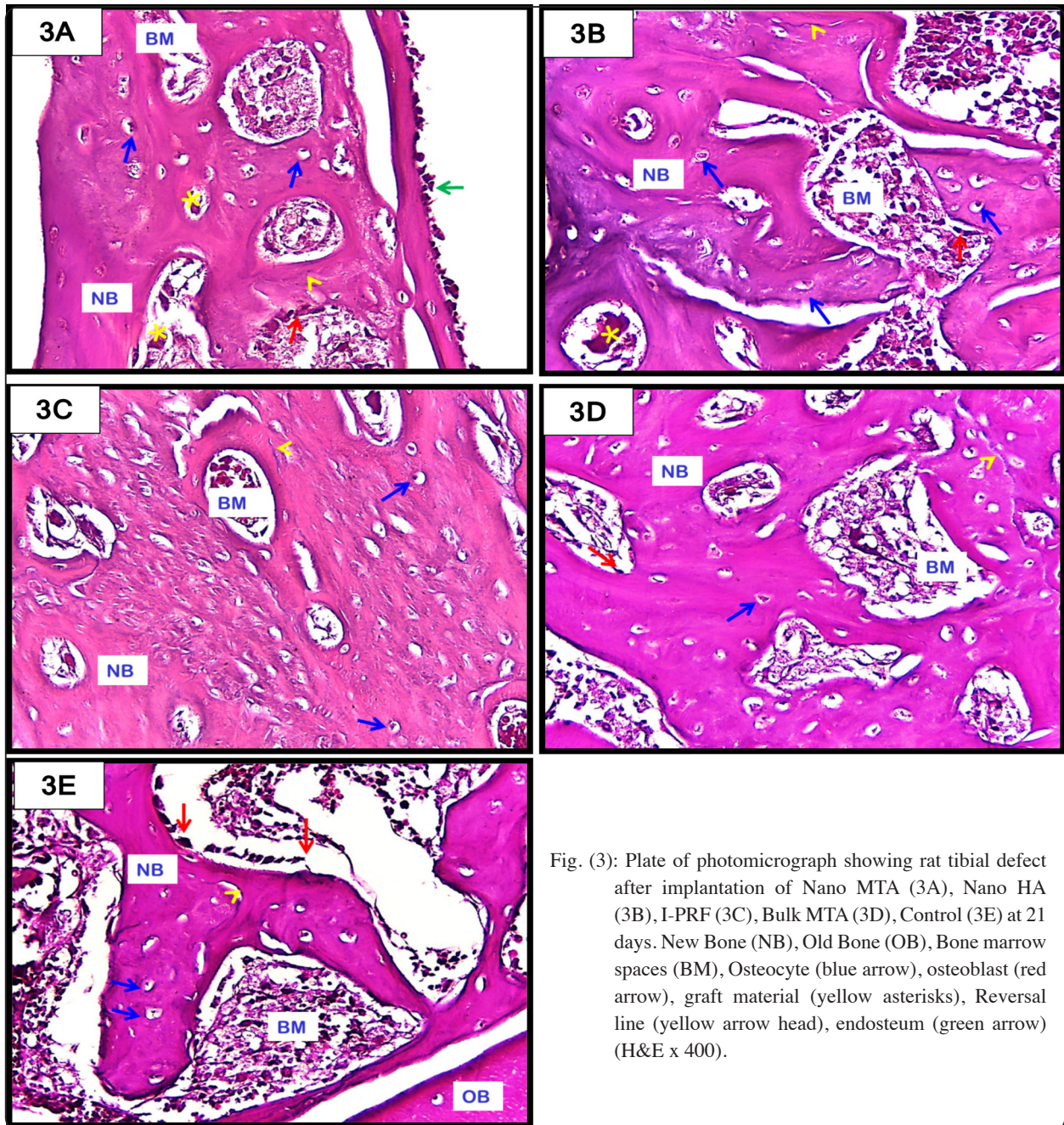
Fig. (3): Plate of photomicrograph showing rat tibial defect after implantation of Nano MTA (3A), Nano HA (3B), I-PRF (3C), Bulk MTA (3D), Control (3E) at 21 days. New Bone (NB), Old Bone (OB), Bone marrow spaces (BM), Osteocyte (blue arrow), osteoblast (red arrow), graft material (yellow asterisks), Reversal line (yellow arrow head), endosteum (green arrow) (H&E x 400).

II) Histomorphometric analysis:

The mean values of the regenerated bone area % during the healing of the bone defects were calculated and demonstrated in Table 1, 2. The histomorphometrical results revealed the regenerated bone area % in bone defects was greatest in the Nano MTA sub-group (50.4078 +/- 3.916, 80.077 +/- 4.605) followed by Nano HA sub-group (44.972 +/- 5.507, 75.032 +/- 6.134), then i-PRF sub-group (42.256 +/- 4.005, 68.562 +/- 4.666), after that Bulk MTA sub-group (38.051 +/- 5.753, 60.17 +/- 4.729), the least percentage was recorded in control sub-group (28.997 +/- 2.858, 45.002 +/- 4.262) in 7 days and 21 days respectively. There was no significant difference between Nano MTA and Nano HA (P>0.05). However, there

was significant difference between Nano MTA and i-PRF sub-groups (P<0.01). Whereas, there was extreme significant difference between the Nano MTA sub-group and the Bulk MTA sub-group (P<0.001) in both time intervals. There was significant difference between i-PRF and Bulk MTA sub-group at both time intervals (P<0.05). Likewise, significant difference was noted between Nano HA sub-group and Bulk MTA sub-group (P<0.01) at 7

days and (P<0.05) at 21 days. Statistically important differences were found between bone formations in all treated sub-groups (A-D) in comparison with the untreated control sub-group in both interval times (P<0.001). However, an increase in the bone area % was observed throughout the experimental periods in all sub-groups without statistical difference Table 2, Fig. 4

TABLE (1) Mean and standard deviation of bone area percentages in all sub-groups at 7 and 21 days.

Sub-groups	Time intervals	
	7 days	21 days
	Mean +/- SD	
Nano MTA	50.4078 +/- 3.916	80.077 +/- 4.605
Nano HA	44.972 +/- 5.507	75.032 +/- 6.134
i-PRF	42.256 +/- 4.005	68.562 +/- 4.666
Bulk MTA	38.051 +/- 5.753	60.17 +/- 4.729
Control	28.997 +/- 2.858	45.002 +/- 4.262

Fig. (4) Graph representing the comparison of the mean of bone area percentage for all sub-groups at 7 and 21 days.

TABLE (2) Comparing Mean Differences and P value of bone area percentage in all subgroups at 7 and 21 days.

Sub-groups	Time intervals			
	7 days		21 days	
	Mean difference	P value	Mean difference	P value
Nano MTA vs Nano HA	5.435	ns P>0.05	5.045	ns P>0.05
Nano MTA vs i-PRF	8.152	** P<0.01	10.515	** P<0.01
Nano MTA vs Bulk MTA	12.356	*** P<0.001	19.906	*** P<0.001
Nano MTA vs Control	21.410	*** P<0.001	35.075	*** P<0.001
Nano HA vs i-PRF	2.717	ns P>0.05	4.089	ns P>0.05
Nano HA vs Bulk MTA	9.451	** P<0.01	12.861	** P<0.05
Nano HA vs Control	13.258	*** P<0.001	30.03	*** P<0.001
i-PRF vs Bulk MTA	6.921	* P<0.05	8.392	* P<0.05
i-PRF vs Control	15.975	*** P<0.001	23.56	*** P<0.001
Bulk MTA vs Control	9.054	*** P<0.001	15.168	*** P<0.001

DISCUSSION

Bone defect treatment resulted from trauma, tumor or infection has always been a difficult problem in the medical domain. The conventional treatment approach for bone defects comprises bone grafting, which is a surgical procedure that uses patient's own bone (autograft), removed from another location like hip or ribs or from a human donor (allograft) to fill up the defect. However, the limited amounts of bone that can be safely obtained together with the risk of donor site morbidity limit the applicability of this approach [22]. Therefore, an alternative strategy for bone grafting is required in the form of synthetic materials that can promote bone regeneration. A large variety of synthetic materials for bone substitution have already been investigated for this purpose [23]. Moreover, natural biomaterials can be used as a bone substitute for bone regeneration as injectable platelet rich fibrin; which is obtained using a modified centrifugation protocol that produces a 1 mL layer of i-PRF that is utilized in a liquid formulation preceding fibrin clot formation (coagulation) without having to use anti-coagulants; thereby being 100% naturally-derived [24]. The aim of this study was to assess and compare bone regenerative capacity of Nano MTA, Nano HA, i-PRF and Bulk MTA in accelerating bone formation in surgically created bone defects in albino rats through histological and histomorphometric examination after seven and 21 days.

In the present study, white albino rats were used as they are easy to handle and less expensive. In addition, breeding cycles are substantially shorter, providing enough animals for large study groups in a reasonable amount of time [25]. In addition, male rats were used in this research, as females are often avoided regarding their estrogen status which might be a limiting factor when using these animals in fracture healing studies [26].

For proper evaluation of bone regeneration, tibia was chosen in the ongoing study. It is considered a beneficial surgical site as it is not affected by bacterial infection and trauma from chewing. Also, the double layer suturing (first deep soft tissue and then the skin) prevents unwanted wound site exposure which might accelerate the recovery process [27].

In general, the results revealed that all the tested materials were capable of bone regeneration throughout the experiment. Noteworthy, Nano MTA demonstrated superior results compared to other materials. However, this superiority compared to Nano HA was with no statistical significant difference.

Nano MTA and Nano HA sub-groups revealed greater bone regenerative capacity expressed in higher bone area % with statistical significant difference compared to Bulk MTA sub-group in the two time periods of the study. This might be due to Nano MTA and Nano HA had larger surface area compared to Bulk MTA; therefore, its ability to release Ca^{2+} and OH ions was enhanced. These effects help Nano-sized materials achieve higher pH values in early stages of hydration, resulting in decreased macrophage and osteoclast counts [28, 29]. This is in accordance with earlier published results when powder nano-modification was performed to calcium silicate-based cement; enhanced the favorable tissue response and osteogenesis properties of MTA based materials [30].

Interestingly, the osteoinductivity, osteoconductivity and biocompatibility of HA are well studied [31, 32]. When HA is in nano-size (Nano HA), similar to native HA in bone, these properties are enhanced. Nano HA has a positive effect on protein adhesion, cell adhesion and proliferation [33, 34]. Also, Nano HA has osteogenic potential as it can release calcium and phosphorus ions, which are involved in bone regeneration [35]. Our study has shown new bone apposition in the defects filled with Nano HA. Bone defects and the spaces between the grafted material residues were filled with newly formed bone and well-vascularized connective tissue. Investigation of the healing of a nano-crystalline synthetic

HA demonstrated sprouting vessels from pre-existent host vessels entering the un-degraded granules. Later, these vessels form an intergranular network which probably transports osteoblastic precursor cells into the granules [36]. This may be relevant for osteoconductive and probably also osteoinductive features of HA leading to early osteogenesis, and subsequent remodeling of the newly formed bone [37]. Moreover, Nano HA gradient coating on implants was bioactively able to enhance implant osteointegration by promoting bone formation and delaying the bone absorption around the materials [38].

Bulk MTA revealed least bone area % compared to all experimental sub-groups, but statistically significant higher bone area % than control subgroup. Bulk MTA has the tendency catalyze in the presence of tissue fluids and releases all its cationic content, of which calcium has the highest proportion [39]. Nonetheless, nano-modification of bulk MTA increased its surface area which resulted in compositional changes in the vicinity of tissues. This might explain the extreme statistical significant difference between Nano MTA sub-group and Bulk MTA sub-group in both 7and 21 day time intervals. The results of tested group materials of current study are consistent with previous studies [30, 35, 38, 40 & 41].

i-PRF has been introduced with the aim of delivering to clinicians an easy to use platelet concentrate in liquid formulation which can be either utilized alone or combined easily with various biomaterials. Taking advantage of slower and shorter centrifugation speeds, a higher presence of regenerative cells with higher concentrations of growth factors can be observed when compared to other formulations of PRF utilizing higher centrifugation speeds as highlighted by our group's previous research [42, 43]. The histological findings demonstrated that i-PRF-treated defects presented an accelerated material degradation compared to all materials used and enhanced newly bone formation with higher values of bone area % compared to Bulk MTA and control sub-groups.

i-PRF has the ability to influence osteoblast cell behavior via influencing the migration, proliferation and differentiation of human osteoblasts. It should be noted that the beneficial effect of i-PRF is due to the additional incorporation of leukocytes besides fibrin proteins that have benefit to coagulate [24]. Furthermore, with time, i-PRF form a small clot as a result of its fibrin components that act as a dynamic gel with cells contained within its hydrogel. Therefore, it was hypothesized that even following 10 days; an additional release of growth factors could still be expected from i-PRF [44]. However, it remains a challenge for researchers in regenerative dentistry field to further understand the potential of platelet formulation on osteogenesis and to further explore their regenerative potential by fully revealing their added advantages/ disadvantages.

Furthermore, it was found that the bone formation was increased in treated bony defects compared to untreated ones with no statistical significant difference. This highlights the need for another late sacrifaction date in this experiment.

The results of current study suggested that bone regeneration was enhanced by reducing the particle size (nano-modified). As the highest percentages were recorded in Nano MTA and Nano HA subgroups this was in agreement with a previous investigation [30]. Also i-PRF induces the formation of bone but when comparing it with Nano MTA and Nano HA, it showed lesser bone formation; this may be due to its liquid form decreases its ability to be stabilized in the bony defect compared with the other materials but it still has a better results compared with Bulk MTA.

CONCLUSION

Within the limitations of the present experiments, it could be concluded that Nano MTA induced the most favorable tissue response and osteopromotion properties followed by Nano HA and i-PRF compared with conventional MTA. This may be attributed to the similarities between the Nano

MTA and the natural bone in composition and the particle size, which play an important role in stimulating osteoblasts, and favor faster release rate of Ca^{2+}. Although the results are very encouraging, more studies on enlightening i-PRF properties are mandatory before routine clinical use.

REFERENCES

1. Castellucci A.: The use of mineral trioxide aggregate in clinical and surgical endodontics. Dent Today. 2003; 22:74–81.

2. Torabinejad M., Hong C.U., Lee S.J., Monsef M., Pitt Ford T.R.: Investigation of mineral trioxide aggregate for root end filling in dogs. J. Endod. 21:603, 1995.

3. Okiji T., Yoshiba K.: Reparative dentinogenesis induced by mineral trioxide aggregate: a review from the biological and physicochemical points of view. Int J Dent. 2009;2009:464280.

4. Oviir T., Pagoria D., Ibarra G., Geurtsen W.: Effects of gray and white mineral trioxide aggregate on the proliferation of oral keratinocytes and cementoblasts. J. Endod 2006;32:210–3.

5. Al-Rabeah E., Perinpanayagam H., MacFarland D.: Human alveolar bone cells interact with ProRoot and tooth-colored MTA. J. Endod 2006;32:872-5.

6. Josette C.: The chemical composition of mineral trioxide aggregate. JCD. 2008;11:141-3.

7. Kubasiewicz-Ross P., Hadzik J., Seeliger J., Kozak K., Jurczyszyn K., Gerber H., Dominiak M., Kunert-Keil C.: New nano-hydroxyapatite in bone defect regeneration: A histological study in rats. Ann Anat. 2017;213:83–90.

8. Giannoudis P.V., Dinopoulos H., Tsiridis E.: Bone substitutes: an update. Injury 2005; 36:20-7.

9. LeGeros R.Z.: Properties of osteoconductive biomaterials: calcium phosphates. Clin Orthop Relat Res 2002;395,81-98.

10. Chogle S., Kinaia B., Goodis H.: Nanobiomaterials in Clinical Dentistry (Second Edition). Chapter 21 - Scope of nanotechnology in endodontics. 2019:517-39.

11. Ghanaati S, Booms P, Orlowska A, et al. Advanced platelet-rich fibrin: a new concept for cell-based tissue engineering by means of inflammatory cells. J Oral Implantol. 2014;40:679-689.

12. Patidar S., Kalra N., Khatri A., Tyagi R.: Clinical and radiographic comparison of platelet-rich fibrin and mineral trioxide aggregate as pulpotomy agents in primary molars. J Indian Soc Pedod Prev Dent. 2017;35:367–73.

13. Lv H., Chen Y., Cai Z., Zhang M., Zhou R., Huang X.: The efficacy of platelet-rich fibrin as a scaffold in regenerative endodontic treatment: a retrospective controlled cohort study. BMC Oral Health. 2018;18:139.

14. Do Lago ES., Ferreira S., Garcia IR Jr., Okamoto R., Mariano RC.: Improvement of bone repair with l-PRF and bovine bone in calvaria of rats. histometric and immuno-histochemical study. Clin Oral Investig. 2019;10.1007/s00784-019-03018-4.

15. Varela HA, Souza JCM, Nascimento RM, et al. Injectable platelet rich fibrin: cell content, morphological, and protein characterization. Clin Oral Investig. 2019;23:1309-1318.

16. Fujioka-Kobayashi M, Miron RJ, Hernandez M, Kandalam U, Zhang Y, Choukroun J. Optimized Platelet-Rich Fibrin With the Low-Speed Concept: Growth Factor Release, Biocompatibility, and Cellular Response. J Periodontol. 2017;88:112-121.

17. Kobayashi E, Flückiger L, Fujioka-Kobayashi M, et al. Comparative release of growth factors from PRP, PRF, and advanced-PRF. Clin Oral Investig. 2016;20:2353-2360.

18. Miron RJ, Fujioka-Kobayashi M, Hernandez M, et al. Injectable platelet rich fibrin (i-PRF): opportunities in regenerative dentistry?. Clin Oral Investig. 2017;21:2619-2627.

19. Atalay Y, Bozkurt MF, Gonul Y, et al. The effects of amlodipine and platelet rich plasma on bone healing in rats. *Drug Des Devel Ther*. 2015;9:1973-1981.

20. Abràmoff MD, Magalhães PJ, Ram SJ. Image processing with ImageJ. Biophotonics international. 2004;11:36-42.

21. Ferreira T, Rasband W. ImageJ user guide. IJ1 46r Natl Inst Health, Bethesda. 2012.

22. Hing KA. Bone repair in the twenty–first century: biology, chemistry or engineering?. Philosophical Transactions of the Royal Society of London. Series A: Mathematical, Physical and Engineering Sciences. 2004 Dec 15; 362(1825):2821-50.

23. Bongio M, Van Den Beucken JJ, Leeuwenburgh SC, Jansen JA. Development of bone substitute materials: from 'biocompatible'to 'instructive'. Journal of Materials Chemistry. 2010;20(40):8747-59.

24. Xuzhu Wang, Yufeng Zhang, Joseph Choukroun, Shahram Ghanaati, Richard J Miron. Effects of an injectable platelet-rich fibrin on osteoblast behavior and bone tissue formation in comparison to platelet-rich plasma. Platelets. 2018 Jan;29(1):48-55.

25. Histing T, Garcia P, Holteins JH et al . Small animal bone healing models: standards, tips, and pitfalls results of a consensus meeting. Bone 2011; 49(4):591–599

26. McCann, R. M., Colleary, G., Geddis, C., Clarke, S. A., Jordan, G. R., Dickson, G. R., & Marsh, D. (2008). Effect of osteoporosis on bone mineral density and fracture repair in a rat femoral fracture model. Journal of Orthopaedic Research, 26, 384–393.

27. Gholami, G. A., Tehranchi, M., Kadkhodazadeh, M., Moghadam, A. A., Ghanavati, F., Ardakani, M. R. T., Aghaloo, M., & Mashhadiabbas, F. (2010). Histologic and histomorphometric evaluation of bone graft substitutes in experimental defects. Res. J. Biol. Sci. 5, 465-469.

28. Mankani MH, Kuznetsov SA, Fowler B, Kingman A, Robey PG. In vivo bone formation by human bone marrow stromal cells: effect of carrier particle size and shape. Biotechnol Bioeng. 2001;72:96- 107.

29. Watari F, Takashi N, Yokoyama A, Uo M, Akasaka T, Sato Y, et al. Material nanosizing effect on living organisms: non-specific, bio-interactive, physical size effects. J R Soc Interface. 2009;6:371-88.

30. Saghiri MA, Orangi J, Tanideh N, Asatourian A, Janghorban K, Garcia-Godoy F, Sheibani N. Repair of bone defect by nano-modified white mineral trioxide aggregates in rabbit: A histopathological study. Medicina oral, patologia oral y cirugia bucal. 2015 Sep;20(5):e525.

31. Lin L, Chow KL, Leng Y. Study of hydroxyapatite osteoinductivity with an osteogenic differentiation of mesenchymal stem cells. J Biomed Mater Res A. 2009;89(2):326-335. doi:10.1002/jbm.a.31994.

32. Teotia, A. K.; Gupta, A.; Raina, D. B.; Lidgren, L.; Kumar, A. Gelatin-Modified Bone Substitute with Bioactive Molecules Enhance Cellular Interactions and Bone Regeneration. ACS Appl. Mater. Interfaces 2016, 8, 10775–10787.

33. Garagiola, U., Grigolato, R., Soldo, R., Bacchini, M., Bassi, G., Roncucci, R., De Nardi, S., 2016. Computer-aided design/computer-aided manufacturing of hydroxyapatite scaffolds for bone reconstruction in jawbone atrophy: a systematic review and case report. Maxillofac Plast Reconstr Surg 38, 2.

34. Teotia, A.K., Raina, D.B., Singh, C., Sinha, N., Isaksson, H., Tagil, M., Lidgren, L., Kumar, A., 2017. Nano-Hydroxyapatite Bone Substitute Functionalized with Bone Active Molecules for Enhanced Cranial Bone Regeneration. ACS Appl Mater Interfaces 9, 6816-6828.

35. Wang H, Li Y, Zuo Y, Li J, Ma S, Cheng L. Biocompatibility and osteogenesis of biomimetic nano-hydroxyapatite/polyamide composite scaffolds for bone tissue engineering. Biomaterials. 2007;28:3338-48.

36. Gotz, W., Gerber, T., Michel, B., Lossdorfer, S., Henkel, K.O., Heinemann, F., 2008. Immunohistochemical characterization of nanocrystalline hydroxyapatite silica gel (NanoBone(r)) osteogenesis: a study on biopsies from human jaws. Clin Oral Implants Res 19, 1016-1026.

37. Gotz, W., Lenz, S., Reichert, C., Henkel, K.O., Bienengraber, V., Pernicka, L., Gundlach, K.K., Gredes, T., Gerber, T., Gedrange, T., Heinemann, F., 2010. A preliminary study in osteoinduction by a nano-crystalline hydroxyapatite in the mini pig. Folia Histochem Cytobiol 48, 589-596.

38. Xie XH, Yu XW, Zeng SX, Du RL, Hu YH, Yuan Z, et al. Enhanced osteointegration of orthopaedic implant gradient coating composed of bioactive glass and nanohydroxyapatite. Mater Sci Mater Med. 2010;21:2165-73.

39. Sarkar N, Caicedo R, Ritwik P, Moiseyeva R, Kawashima I. Physicochemical basis of the biologic properties of mineral trioxide aggregate. J Endod. 2005;31:97-100.

40. Watari F, Takashi N, Yokoyama A, Uo M, Akasaka T, Sato Y, et al. Material nanosizing effect on living organisms: non-specific, bio-interactive, physical size effects. J R Soc Interface. 2009;6:371-88.

41. Koh ET, Torabinejad M, Pitt Ford TR, Brady K, McDonald F. Mineral trioxide aggregate stimulates a biological response in human osteoblasts. J Biomed Mater Res. 1997;37:432-9.

42. Ghanaati S, Booms P, Orlowska A, Kubesch A, Lorenz J, Rutkowski J, Landes C, Sader R, Kirkpatrick C, Choukroun J (2014) Advanced platelet-rich fibrin: a new concept for cell-based tissue engineering by means of inflammatory cells. The Journal of oral implantology 40:679–689. doi:10.1563/aaid-joi-D-14-00138

43. Fujioka-Kobayashi M, Miron RJ, Hernandez M, Kandalam U, Zhang Y, Choukroun J (2016) Optimized platelet rich fibrin with the low speed concept: growth factor release, biocompatibility and cellular response. J Periodontol:1–17. doi:10.1902/jop.2016. 160443

44. Miron RJ, Fujioka-Kobayashi M, Hernandez M, Kandalam U, Zhang Y, Ghanaati S, Choukroun J. Injectable platelet rich fibrin (i-PRF): opportunities in regenerative dentistry?. Clinical oral investigations. 2017 Nov 1;21(8): 2619-27.